Journal of Physics: Conference Series **2446** (2023) 012054 doi:10.1088/1742-6596/2446/1/012054

$K_L^0 \to \gamma + dark\ photon(\bar{\gamma})$ Search at the J-PARC KOTO Experiment

Tong Wu

Department of Physics, National Taiwan University, Taipei, Taiwan 10617 Republic of China

E-mail: tong@hep1.phys.ntu.edu.tw

Abstract. We present the study of massless dark photons in the decay of $K_L^0 \to \gamma\bar{\gamma}$ in the J-PARC KOTO experiment. The massless dark photon ($\bar{\gamma}$) is different from the massive dark photon because it does not mix directly with ordinary photons, but it could interact with SM particles through direct coupling with quarks. In some theoretical predictions, the $\mathcal{BR}(K_L^0 \to \gamma\bar{\gamma})$ can be as large as $\mathcal{O}(10^{-3})$, which is well within the sensitivity of KOTO. Because of the lack of kinematic constraints, searching for $K_L^0 \to \gamma\bar{\gamma}$ could be challenging, but the hermetic veto system of KOTO provides a unique opportunity to probe for this decay. We used three techniques to suppress the neutron background, based on machine learning, Fourier analysis, and both-end readout. We will present the background suppression result based on data collected in 2020.

1. Introduction

The dark sector has been explored in high energy physics. Many experiments are searching for the massive dark photon (A') but nothing has been observed so far. That turns our interest to search for another type of dark photon, the massless dark photon. The massless dark photon ($\bar{\gamma}$) is different from the massive one because it has no direct mixing with the ordinary photon. Several massless dark photon decay modes are possible and were explored in the KOTO experiment: one of these is $K_L^0 \to \gamma\bar{\gamma}$. In some theoretical predictions, the $\mathcal{BR}(K_L^0 \to \gamma\bar{\gamma})$ can be enhanced to $\mathcal{O}(10^{-3})$[1], which is well within the sensitivity of KOTO.

2. KOTO Detector at J-PARC

KOTO experiment aims to search for the rare kaon decay $K_L^0 \to \pi^0\nu\bar{\nu}$. The single event sensitivity for the $K_L^0 \to \pi^0\nu\bar{\nu}$ was estimated to be 7.2×10^{-10} in recent results[2]. The cross-sectional view of the KOTO detector is shown in figure 1. The detector measures the photon energy and timing with an electromagnetic calorimeter (CSI) with a radius of 950 mm and a depth of 500 mm, which is comprised of 2716 undoped cesium iodide crystals (CsI). The kaon decay volume is surrounded by a hermetic veto system. This brought KOTO to an excellent position to hunt rare decay processes of neutral kaons with missing energies, such as dark photon searches.

3. Signal: $K_L^0 \to \gamma\bar{\gamma}$

For this study, we took a 2-hour special run with a single-cluster trigger in 2020, with approximately 9.14×10^9 K_L decays. The signal signature of $K_L^0 \to \gamma\bar{\gamma}$ is only one photon

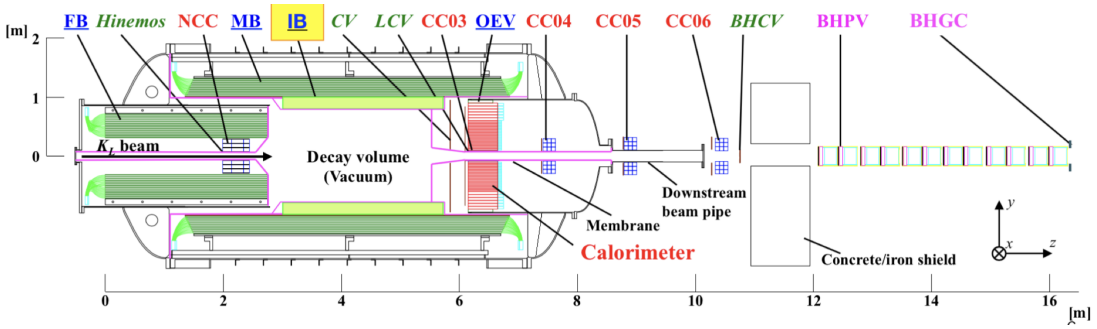

Figure 1. Cross-sectional view of the KOTO detector.

cluster in CSI with no in-time hit in the rest of the detector. We have only two kinematic variables, one is the cluster energy (E) and the other is the distance between the hit position and the center of the CsI (R). The lack of kinematic constraints will be the challenge of this study. A region enclosed by 300 mm $< R <$ 850 mm and 800 MeV $< E <$ 3000 MeV as shown in figure 2 is the signal region.

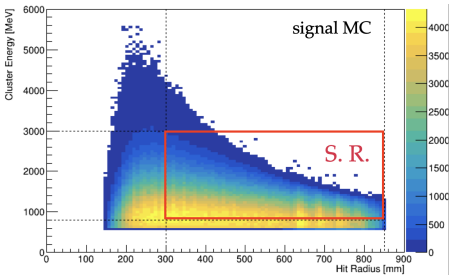

Figure 2. $E - R$ distribution of signal simulation. The red frame indicates the signal region.

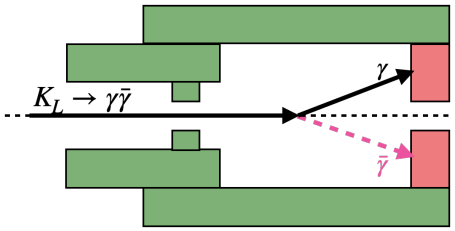

Figure 3. sketch of the $K_L^0 \to \gamma\bar{\gamma}$ event. Only one cluster is observed on the calorimeter.

4. Background

There are two background sources in this analysis: Kaon decay and Neutron cluster.

4.1. Kaon decay background

The primary kaon decay background is $K_L \to 2\gamma$ decay with one missing photon, as shown in figure 4. The estimation of the number of $K_L \to 2\gamma$ background events in the signal region is 1.5 ± 0.4. The other kaon decay backgrounds are shown in table 1. If we assume the $\mathcal{BR}$ to be $\mathcal{O}(10^{-3})$, the number of signal events inside the signal region is $\mathcal{O}(10^5)$. That means the Kaon decay background is negligible in this study.

4.2. Neutron cluster background

Neutron cluster background is the dominant background in this study. The mechanism is that a neutron enters the calorimeter with only one cluster hit, as illustrated in figure 5. We have three tools to suppress the neutron background: cluster shape discrimination with deep learning (CSDDL), pulse shape discrimination by using Fourier analysis (FPSD), and a shower depth measurement.

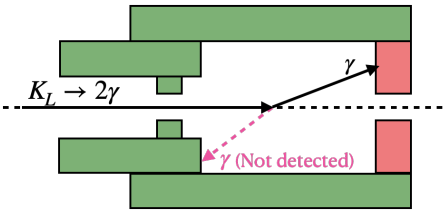

Figure 4. Sketch of the $K_L \to 2\gamma$ event. One photon is missing.

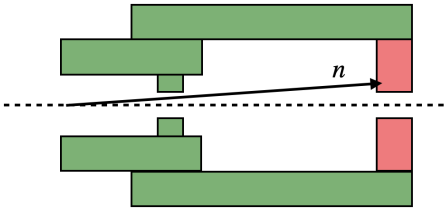

Figure 5. Sketch of the Neutron cluster event.

Cluster Shape Discrimination with Deep Learning (CSDDL) Neutrons and photons have different cluster shape patterns. We use Convolutional Neural Network (CNN) to classify the photon and neutron cluster patterns. Figure 7 shows the performance of CSDDL.

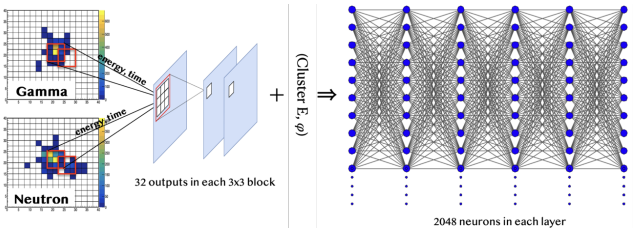

Figure 6. The architecture of CSD neural network training process.

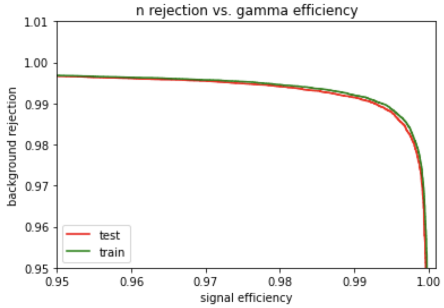

Figure 7. The performance of CSDDL. The x-axis shows the acceptance of photon and the y-axis shows the rejection of neutron

The figure 8 shows the architecture of the training process. The output is between 0 and 1, as shown in the figure 8. We cut on the CSDDL to accept 90% of photons, which rejected 98.5% of neutrons.

Fourier transform for Pulse shape discrimination (FPSD) The difference in shower development also manifests in the pulse shape difference. FPSD discriminated the neutron cluster and photon clusters based on the shape of the ADC waveform. We applied FTT to the ADC raw pulse, then extracted the differences between the neutron and photon in the frequency domain. Figure 9 shows the likelihood ratio. By requiring the 90% signal acceptance, the neutron cluster background rejection efficiency is 89.6%.

Shower-depth The radiation length for photons is shorter than the interaction length for neutrons, resulting in different shower depths in the calorimeter for photons and neutrons. Multi-pixel photon counters (MPPC) were installed in front of the CSI calorimeter, to get the timing difference(ΔT) between PMT and MPPC as shown in figure 10. The distribution of ΔT is shown in figure 11. By requiring ΔT to be less than 29.5 ns, the background rejection efficiency is 84% with a signal loss of 9%.

After applying all these selections mentioned above, the number of neutron cluster background events is suppressed to 28.1 ± 2.4 in the signal region with a rejection efficiency of 99.824%.

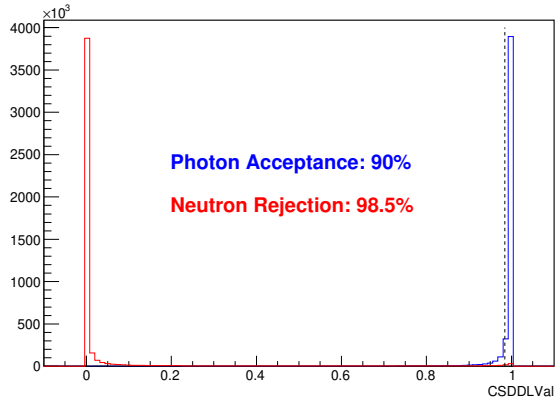

Figure 8. Distribution of the output of CSDDL for hadronic cluster events (red) and photon cluster events (blue). The photon cluster events are obtained through the $K_L^0 \to \gamma\bar{\gamma}$ decay of Monte Carlo. The neutron sample is obtained from neutron data. Closer to 1 means more neutron-like, while the opposite is more photon-like.

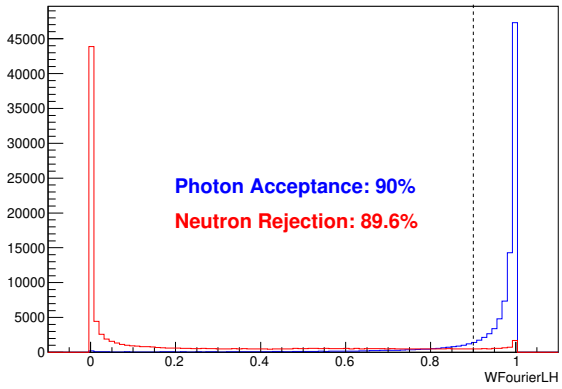

Figure 9. Distribution of the likelihood ratio for hadronic cluster events (red) and photon cluster events (blue).The photon cluster events are obtained through the $K_L^0 \to 3\pi^0$ decay analysis of data. The neutron sample is obtained from neutron data.

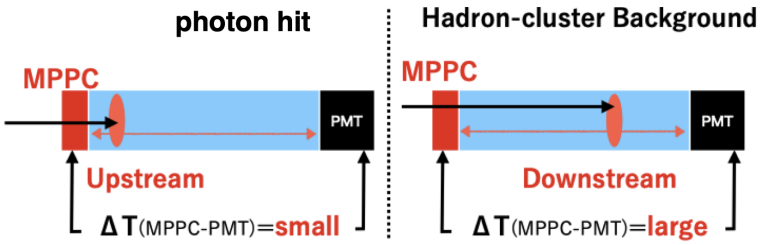

Figure 10. Illustration of shower depth means. An MPPC is installed on the upstream side. The time difference between the photon arriving upstream and downstream ($\Delta T = T_{MPPC} - T_{PMT}$) is used to measure the depth of the reaction and distinguish between photon events (left) and neutron events (right).

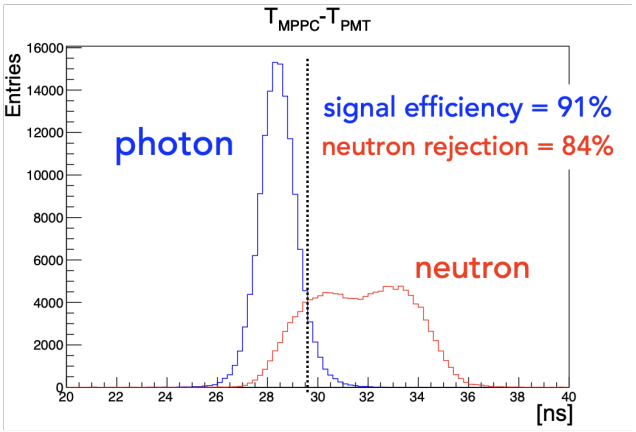

Figure 11. Distribution of the ΔT for neutron events and photon events. The photon cluster events are obtained through the $K_L^0 \to 3\pi^0$ decay analysis of data. The neutron sample is obtained by scattering neutrons in the beam with an Al plate.

5. Summary

Table 1 shows the summary of the number of events left in the signal region for each background source. The K_L decay background is negligible if we assume the $\mathcal{BR}(K_L^0 \to \gamma\bar{\gamma})$ is $\mathcal{O}(10^{-3})$. The neutron background rejection efficiency is 99.824%. The estimation of the number of neutron background events in the signal region is 28.1 ± 2.4.

Although we have considered some major backgrounds, since the 1-cluster final state is easily triggered, we need to study more sources of background and predict its background levels in the next step.

Table 1. Number of events predicted for each source inside the signal region

Source		Number of events
K_L decay	$K_L \to 2\gamma$	1.5 ± 0.4
	$K_L \to 3\pi^0$	< 2.3 (90% C.L.)
	$K_L \to 2\pi^0$	< 0.4 (90% C.L.)
	$K_L \to \pi^\pm e^\mp \nu_e$	< 1.7 (90% C.L.)
	$K_L \to \pi^\pm \mu^\mp \nu_\mu$	< 2.3 (90% C.L.)
	$K_L \to \pi^+\pi^-\pi^0$	< 1.1 (90% C.L.)
Neutron		28.1 ± 2.4

References

[1] Su J Y and Tandean J 2020 *The European Physical Journal C* **80**
[2] Ahn J K *et al.* (KOTO Collaboration) 2021 *Phys. Rev. Lett.* **126**(12) 121801